One and Two Dimensional Quantum Lattice Algorithms for Maxwell Equations in Inhomogeneous Scalar Dielectric Media. II: Simulations

George Vahala[1], Min Soe[2], Linda Vahala[3], and Abhay K. Ram[4]

[1]Department of Physics, William & Mary, Williamsburg, VA23185
[2]Department of Mathematics and Physical Sciences, Rogers State University, Claremore, OK 74017
[3]Department of Electrical & Computer Engineering, Old Dominion University, Norfolk, VA 12319
[4]Plasma Science and Fusion Center, MIT, Cambridge, MA 02139

Abstract: Long time quantum lattice algorithm (QLA) simulations are performed for the multiple reflection-transmission of an initial electromagnetic pulse propagating normally to a boundary layer region joining two media of different refractive index. For these one dimensional (1D) simulations, there is excellent agreement between x-, y- and z- representations, as well as very good agreement with nearly all the standard plane wave boundary condition results for reflection and transmission off a dielectric discontinuity. In the QLA simulation, no boundary conditions are imposed at the continuous, but sharply increasing, dielectic boundary layers. Two dimensional (2D) QLA scattering simulations in the x-z plane are performed for an electromagnetic pulse interacting with a conical dielectric obstacle for the 8-16 qubit model.

1 Introduction

In Part I we [1] developed the theory for QLA for Maxwell equations in scalar 1D and 2D dielectric inhomogeneous media. Here we will perform QLA simulations to verify that QLA perturbative theory is an excellent Maxwell solver.

In Sec. 2 we consider the multiple reflections and transmissions of a 1D pulse as it propagates from a vacuum into a medium slab of refractive index $n(z) = 2$. The thickness of this dielectric slab is chosen to be considerably greater than the length scale assocaited with the initial Gaussian pulse in that medium. In [2] we developed a 1D QLA simulation for Maxwell equations with a y-dependent dielectric while in [3] we presented QLA simulations for an x-dependent dielectric medium. Here 1D QLA simulations are presented for the z-dependent dielectric medium. For both the x-dependent and y-dependent dielectrics, an 8-qubit representation is sufficient. However, for z-dependent dielectrics one requires a 16-qubit representation. This difference between these representations arises from the fact that the z-component Pauli spin matrix σ_z is diagonal. The collision operator requires the coupling of at least 2 qubits locally at each lattice site in order to get entanglement. This entanglement is then spread throughout the lattice by the streaming operators.

Once having determined these three orthogonal 1D QLA representations we can immediately stitch these representations together to develop both 2D and fully 3D QLA representations of Maxwell equations. In this paper we will perform some 2D QLA simulations for an $8-16$ qubit model for refractive indices $n = n(x, z)$.

2 16-qubit QLA Simulation of Electromagnetic Pulse Incident onto a dielectric slab

Here we present some long time evolution of a z-propagating Gaussian pulse. In [1] we showed that a minimal QLA required at least 16 qubits/node. In particular we shall consider multiple reflections and transmissions at strongly varying dielectric boundary layers with vacuum refractive index $n(z) = 1.0$ for $0 < z < 3700$ and for $4300 < z < 6500$ and refractive index $n(z) = 2$ for $3700 < z < 4300$, as shown in Fig. 1(a). The thin (but continuous) boundary layer regions are around $x = 3700$ and $x = 4300$ and approximately 50 lattice units thick, Fig. 1(b).

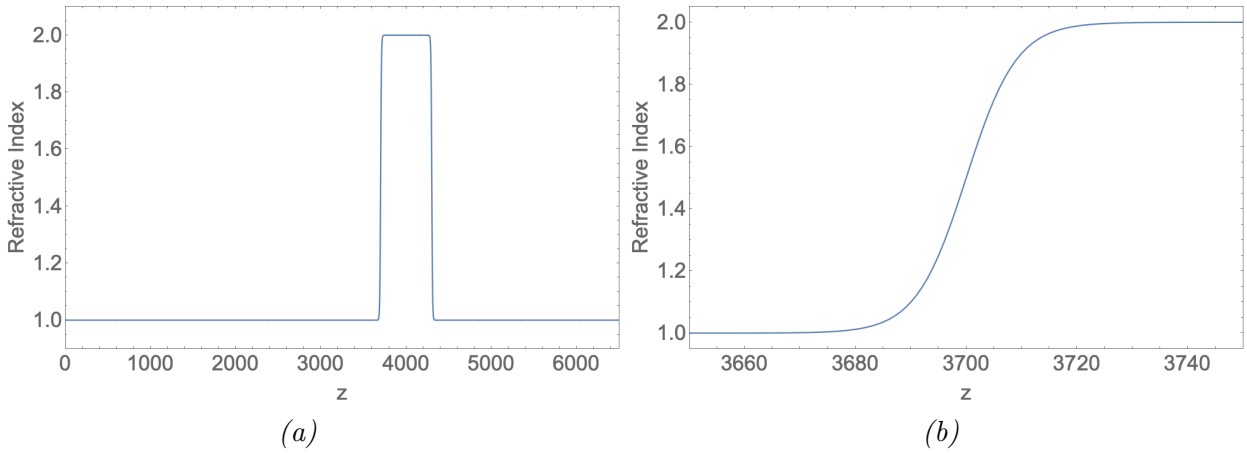

Figure 1: *(a) A localized inhomogeneous dielectric region,* $3700 < z < 4300$ *within a vacuum. (b) a blow-up of the continuous refractive index boundary layer around* $x \approx 3700$.

2.1 Normal incident electromagnetic pulse

The simplest Gaussian vacuum electromagnetic pulse propagating in the z-direction has non-zero components of the electric **E** and magnetic **B** fields

$$E_x(z, t = 0) = 0.01\ exp[-\frac{\epsilon^2(z - z_0)^2}{1500}] = B_y(z, t = 0) \tag{1}$$

where the small parameter $\epsilon = 0.3$ and the initial center of the Gaussian pulse is at $z_0 = 2300$. The half-width of this pulse is about 250 lattice units.

Within the vacuum region, the incident pulse propagates undistorted towards the dielectric slab, as seen in Fig. 2(a) for times $t = 0$, and $t = 4000$. This verifies the QLA perturbative approach does not introduce spurious features into the electromagnetic solution. By $t = 4000$ the forward part of the pulse is just starting to interact with the dielectric boundary layer.

Fig. 2(b) shows a blow-up of the pulse straddling the vacuum-dielectric slab region at time $t = 4800$. Within the dielectric slab, the transmitted pulse has $E_x \neq B_y$, with $max\, B_y = 2\, max\, E_x$.

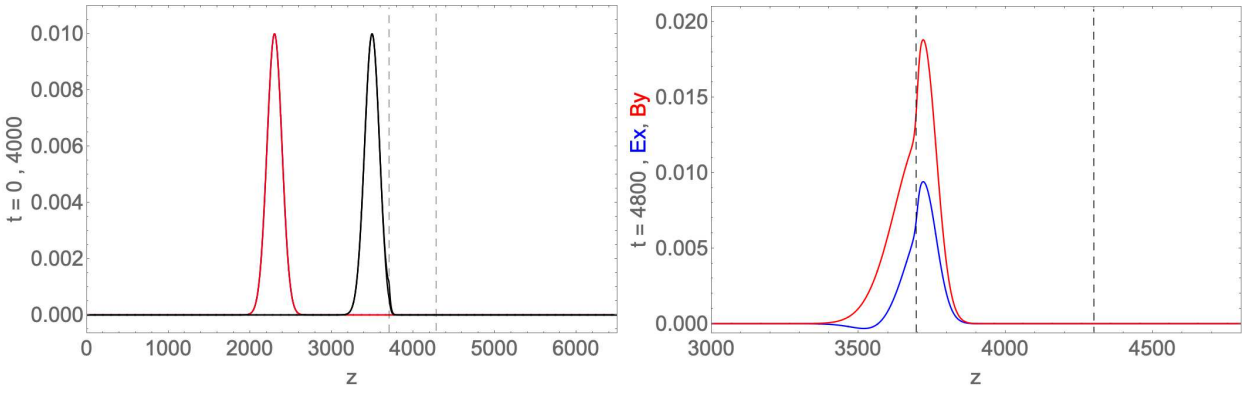

(a) $t = 0$ (red) and $t = 4000$ (black) *(b) $t = 4800$*

Figure 2: *(a) The Gaussian pulse at $t = 0(red)$ and $t = 4000(black)$. In this vacuum region, $E_x = B_y$ and these field components overlay each other.*
(b) At $t = 4800$, there is a partly transmitted pulse within the dielectric slab of $n_{slab} = 2$, and partially reflected pulse back into the vacuum. Because the pulse is moving from vacuum into a higher refractive index region it is the electric field component E_x that exhibits phase change. ($E_x - blue, B_y - red$, dielectric slab lies in $3700 < z < 4300$, its boundaries denoted by the dashed vertical lines).

The part of the pulse in the vacuum is predominantly the transient reflected part with the beginnings of a phase shift in E_x since the reflection is occurring at a low-to-higher refractive index interface.

By $t = 6000$ the transients have died down and one sees the transmitted pulse within the dielectric slab, with $B_y \simeq 2E_x$ and in phase, while the reflected pulse back into the vacuum has E_x π out of phase with B_y. The speed of the transmitted pulse is half that of the incident and reflected pulse in the vacuum (Fig. 3(a)). These results are in complete agreement with the standard plane wave theory [4] of normal reflection from a discontinuous dielectric boundary separating a vacum from a region of refractive index $n = 2$.

By $t = 9000$ the transmitted pulse has reached the right boundary of the dielectric slab and it is undergoing its transmission and reflection at this boundary layer, Fig. 3(b). Since the reflected pulse is now propagating back into a higher refractive medium its B_y-field component undergoes a π phase change.

The time asymptotic state of this stage of pulse evolution is shown in Fig. 4(a) ($t = 10000$). The transmitted pulse ($z > 4300$ is back in the vacuum region so that $E_x \simeq B_y$ and the field components overlay each other, as at t = 0. This pulse has the same speed and width of the initial vacuum pulse, but its amplitude is somewhat reduced (to preserve total energy conservation). The reflected pulse in the dielectric slab is propagating to the left with half the speed of the initial vacuum pulse, with half its width and now with the B_y out-of-phase by π with its E_x field component.

In our simulations we then follow the reflection and transmission of the left-traveling pulse within the dielectric as it hits the inner edge around $z = 3700$. The subsequent transmitted pulse then keeps propagating to the left into the vacuum has its B_y out of phase with its companion E_x. The part of the pulse that is reflected from the dielectric boundary around $z = 3700$ has another $\pi-$ phase change induced in the magnetic field component B_y so that this right traveling pulse within the dielectric has its components again in phase (see Fig. 4(b)), but with $B_y \simeq 2E_x$ within the dielectric region.

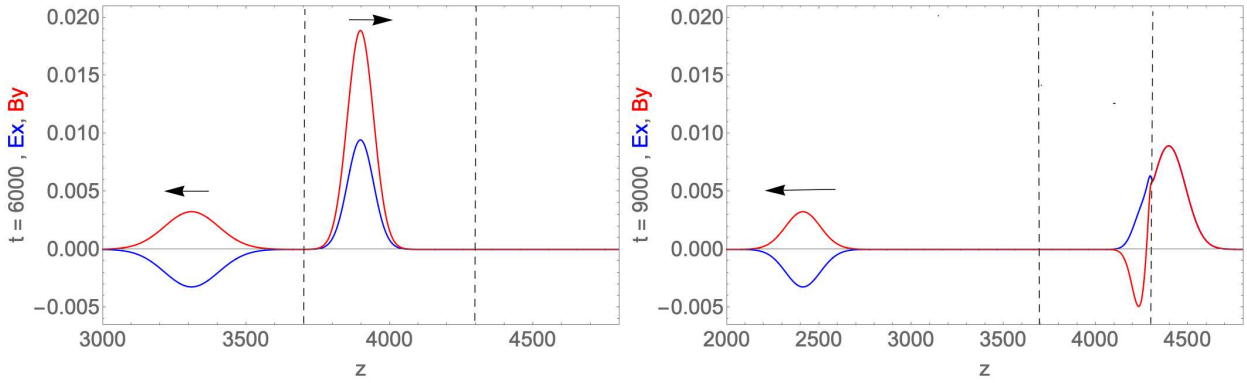

(a) $t = 6000$ *(b) $t = 9000$*

Figure 3: *(a) The reflected and transmitted pulses at time $t = 6000$. Since the initial pulse is incident onto a higher refractive index medium, the reflected E_x undergoes a π phase change, but with $\left|E_x^{refl}\right| = B_y^{refl}$. The transmitted pulse's speed is half of the initial vacuum pulse's, and half the initial pulse width, with $B_y^{trans} \simeq 2E_x^{trans}$.*
(b) At $t = 9000$, the right traveling pulse reaches the right end of the dielectric slab and it itself undergoes transient transmission and reflection. Now, however it is the magnetic field B_y that undergoes a phase change ($E_x - blue, B_y - red$, dielectric slab lies in $3700 < z < 4300$, its boundaries denoted by the dashed vertical lines).

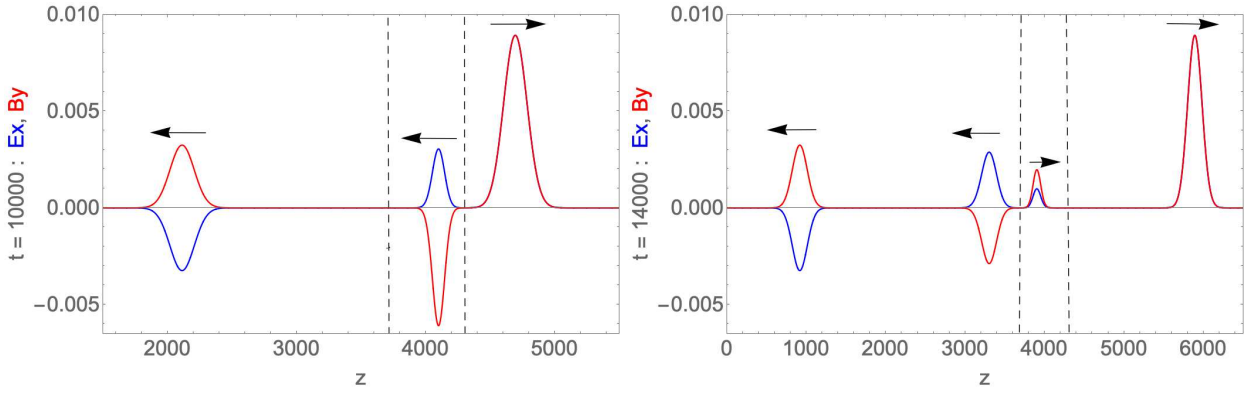

(a) $t = 10000$ *(b) $t = 14000$*

Figure 4: *(a) A quasi-asymptotic state ($t = 10000$) with the first reflection and transmission off the back interface around $z = 4300$. For the reflected pulse in the dielectric slab, it is the magnetic field B_y that undergoes a $\pi-$ phase transition.*
(b) A quasi-asymptotic state ($t = 14000$) following another reflection and transmission off the front interface around $z = 3700$. In the outgoing pulses traveling to the left, the two pulses are out of phase with each other. ($E_x - blue, B_y - red$).

It is interesting to compare the quasi-asymptotic maxima of the E_x and B_y fields during the evolution, Figs. 3(a), 4(a) and 4(b), with those from standard boundary value electromagnetic *plane* wave theory [4]. Note that in the QLA simulations one is time advancing Eq. (49) in Part I [1] which involves a product of mostly unitary but some Hermitian matrices with no boundary conditions applied at any time. For the 1^{st} reflection/transmission from vacuum to dielectric medium of refractive index = 2, from Fig. 3a,

$$QLA \quad Gaussian: \quad \frac{E_{refl}}{E_{inc}} = -0.325 \quad \frac{E_{trans}}{E_{inc}} = 0.944, \quad \frac{B_{refl}}{E_{refl}} = -1.000, \quad \frac{B_{trans}}{E_{trans}} = 2.000 \tag{2}$$

$$EM \quad Plane(b.v.p): \quad \frac{E_{refl}}{E_{inc}} = -0.333 \quad \frac{E_{trans}}{E_{inc}} = 0.667, \quad \frac{B_{refl}}{E_{refl}} = -1.000, \quad \frac{B_{trans}}{E_{trans}} = 2.000 \tag{3}$$

where $b.v.p$ stands for boundary value problem. After the pulse is reflected/transmitted at the back end of the dielectric slab, the quasi-asymptotic maxima are (Fig. 4(s))

$$QLA \quad Gaussian: \quad \frac{E_{refl}}{E_{inc}} = 0.323 \quad \frac{E_{trans}}{E_{inc}} = 0.945, \quad \frac{B_{refl}}{E_{refl}} = -2.000, \quad \frac{B_{trans}}{E_{trans}} = 1.000 \tag{4}$$

$$EM \quad Plane(b.v.p): \quad \frac{E_{refl}}{E_{inc}} = 0.333 \quad \frac{E_{trans}}{E_{inc}} = 1.333, \quad \frac{B_{refl}}{E_{refl}} = -2.000, \quad \frac{B_{trans}}{E_{trans}} = 1.000 \tag{5}$$

After the pulse is reflected/transmitted at the front edge (but from the dielectric side), Fig 4(b)

$$QLA \quad Gaussian: \quad \frac{E_{refl}}{E_{inc}} = 0.323 \quad \frac{E_{trans}}{E_{inc}} = 0.945, \quad \frac{B_{refl}}{E_{refl}} = 2.000, \quad \frac{B_{trans}}{E_{trans}} = -1.000 \tag{6}$$

$$EM \quad Plane(b.v.p): \quad \frac{E_{refl}}{E_{inc}} = 0.333 \quad \frac{E_{trans}}{E_{inc}} = 1.333, \quad \frac{B_{refl}}{E_{refl}} = 2.000, \quad \frac{B_{trans}}{E_{trans}} = -1.000 \tag{7}$$

We see excellent agreement of QLA simulations with plane wave boundary value theory - except in the ratio of transmitted to incident ratios of the electric field. All the phase flipping as one moves either from low to high refractive index, or vice versa, is reproduced by our QLA. The length scales of the pulses and their speeds in the vacuum and dielectric region are fully reproduced by QLA. We feel that this discrepancy with plane wave boundary value theory arises from the difference between a plane wave and a Gaussian pulse.

Finally, in these 1D simulations of the normal incidence of a Gaussian pulse onto a dielectric slab we compute the instantaneous Poynting flux S(t)

$$S(t) = \int_0^L \mathbf{E}(z,t) \times \mathbf{B}(z,t) \cdot \hat{\mathbf{z}} \, dz \tag{8}$$

It is seen from Fig. 5, that QLA conserves energy very well throughout the simulation except during the overlap of incident/reflected pulses around the slab boundaries $z = 3700$ or $z = 4300$. During these time intervals it is very difficult to distinguish which part of the pulse is incident and which part of the pulse is due to reflection – see e.g., Fig. 2(b) (for $t = 4800$) or Fig. 3(b) ($t = 9000$) - thus making the identification of the outward directed normal difficult.

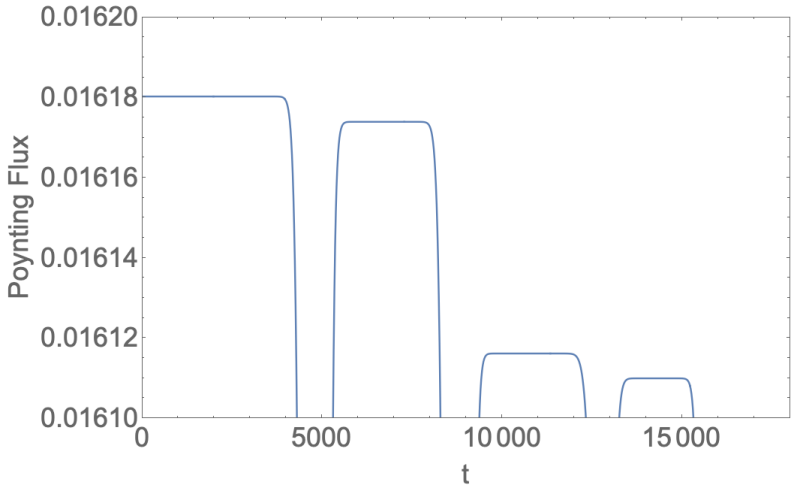

Figure 5: *The instantaneous Poynting flux. The time intervals* $4200 < t < 5300$, $8200 < t < 9300$ *and* $12400 < t < 13300$ *are those in which there is pulse overlap with either the front or the back boundaries of the dielectric slab.*

3 2D QLA Scattering from a Dielectric Obstacle

We perform an 8-16 qubit $x - z$ 2D QLA simulation of a Gaussian pulse propagating in the $x-$direction towards a conical dielectric obstacle (Fig. 6(a)) with the only non-zero field components being E_y and B_z, Fig 6(b). The 2D dielectric cone has a base $75 < x/4 < 225$ and $175 < z/4 < 325$ and with a peak in the refractive index of 3 around $x/4 = 150, z/4 = 255$. The short-time simulations were performed on a 2048×2048 grid, but the data was plotted at every 4th point - hence the figures are drawn on a $0 < x/4, z/4 < 512$ grid. The simulations are valid for relatively short-times since the pulse reaches the computational boundary of 2048^2 relatively quickly.

By $t = 1250$, Fig. 7(a), the Gaussian pulse is interacting with the dielectric cone and develops 2D spatial structure. Since the cone's refractive index is > 1, that part of the Gaussian pulse within the dielectric region slows down within the dielectric (Fig. 7(a)). Figures 7(a)-(f) shows the time evolution of the $E_y(x, z, t)$-field component as the pulse interacts and propagates past the dielectric obstacle. For $z/4 << 175$ and $325 << z/4$ the E_y retains its initial Gaussian-like profile and its vacuum phase velocity. By $t = 5500$, Fig. 7(f), one also sees that a part of the E_y-field consists of an outward propagating circular wavefront emitted from the dielectric cone.

Long-time results are obtained when QLA is run on an 8192^2-grid, Figs 8 (a)-(c). Indeed one sees the outward propagating circular wavefront as though emitted from the dielectric cone. In the primary field components E_y and B_z one also has that part arising from the initial pulse itself, indented by the dielectric obstacle in whcih the pulse propagates with smaller phase velocity than that part propagating in the vacuum (Figs. 8(a)-(b)). The secondary field component B_x is generated by the 2D dielectric obstacle and so does not display any of the pulse geometry seen in the primary field components E_y and B_z. The field B_x exhibits large scale dipole structure (Fig. 8(c)) which is made somewhat clearer by taking a different perspective of the plot, Fig. 8(d).

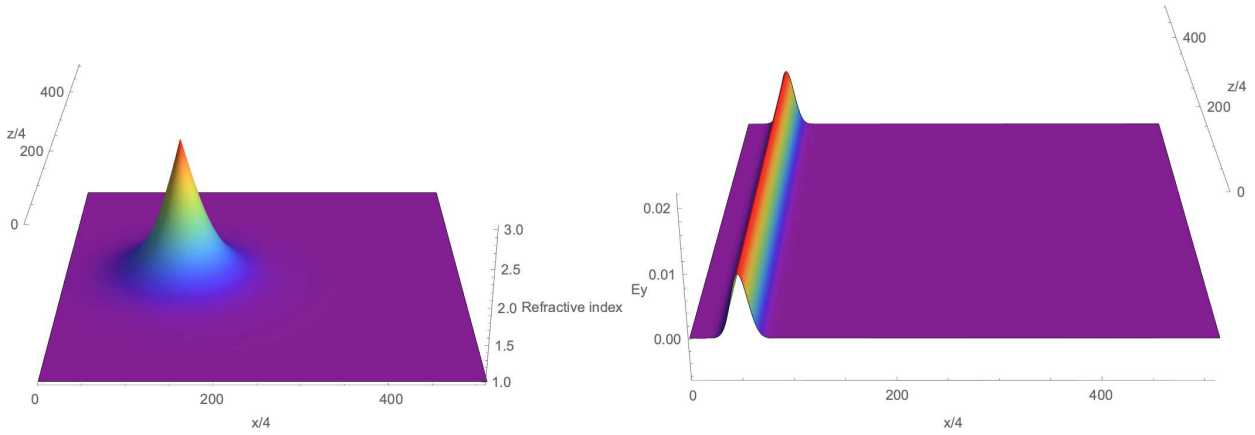

(a) refractive index *(b) $t = 0$ Gaussian pulse*

Figure 6: *(a) The refractive index of a conical dielectric obstacle .*
(b) The initial E_y-field of a Gaussian pulse as it propagates in the $x-$direction. Initially in the vacuum region $E_y = B_z$.

4 Conclusion and Summary

We have presented QLA simulations for multiple 1D reflection/transmission of an electromagnetic pulse incident onto a dielectric slab of thickness significantly greater than the scale length of the pulse. Thus we can follow multiple internal reflections at the front and back boundary layers connecting the dielectric slab to the vacuum. We are looking into the difference between incident plane waves and the Gaussian pulses on the transmitted to incident maxima in the electric field.

From the modular form of the Cartesian coordinates, we investigated the 2D spatial problem of a 1D Gaussian pulse scattering from a dielectric cone for the $8-16$ qubit QLA $x-z$ model. Initially the only non-zero field components of the Gaussian pulse are the E_y and B_z fields with propagation in the $x-$direction. When the 1D pulse interacts with the 2D dielectric cone, B_x field components are generated. We have developed the corresponding $16-16$ qubit model for $x-z$ dependence and preliminary simulations show excellent agreement with the $8-16$ qubit QLA. A 3D full Maxwell QLA solver can now be readily determined. This is currently under investigation.

5 Acknowledgments

LV was partially supported by an AFRL STTR Phase I with Semicyber LLC contract number FA864919PA049. GV, LV and MS were partially supported by an AFRL STTR Phase 2 with Semicyber LLC contract number FA864920P0419. AKR was supported by DoE Grant Number DE-FG02-91ER-54109 and DE-SC0018090. The 2D simulations used resources of the National Energy Research Scientific Computing Center (NERSC), a U.S. Department of Energy Office of Science User Facility operated under Contract No. DE-AC02-05CH11231, as well as the U.S. Department of Defense High Performance Supercomputer at ERDC.

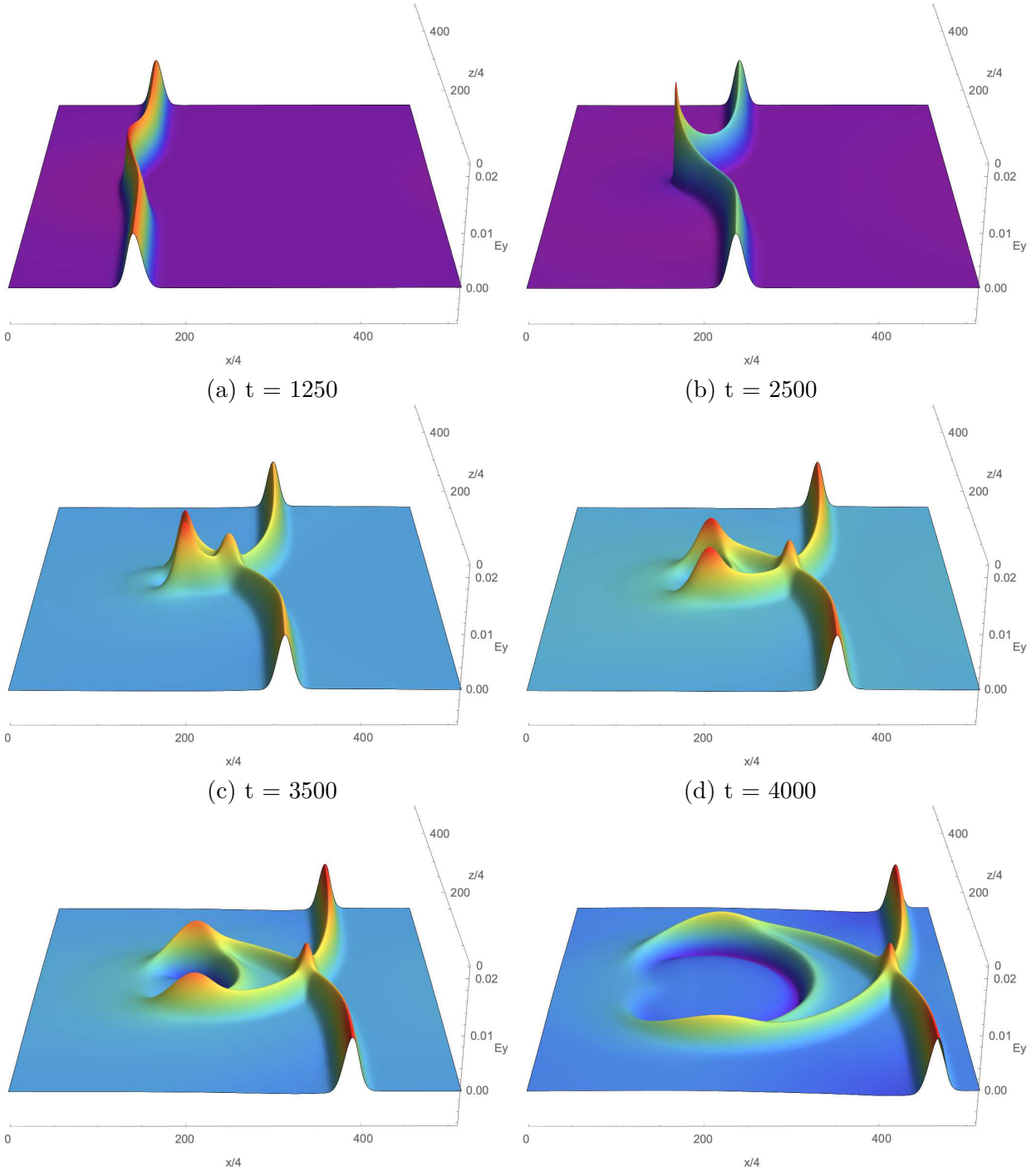

(a) t = 1250

(b) t = 2500

(c) t = 3500

(d) t = 4000

(e) t = 4500

(f) t = 5500

Figure 7: *The evolution of the $E_y(x, z, t)$-component of the electromagnetic pulse as it interacts and propagates past the dielectric cone*

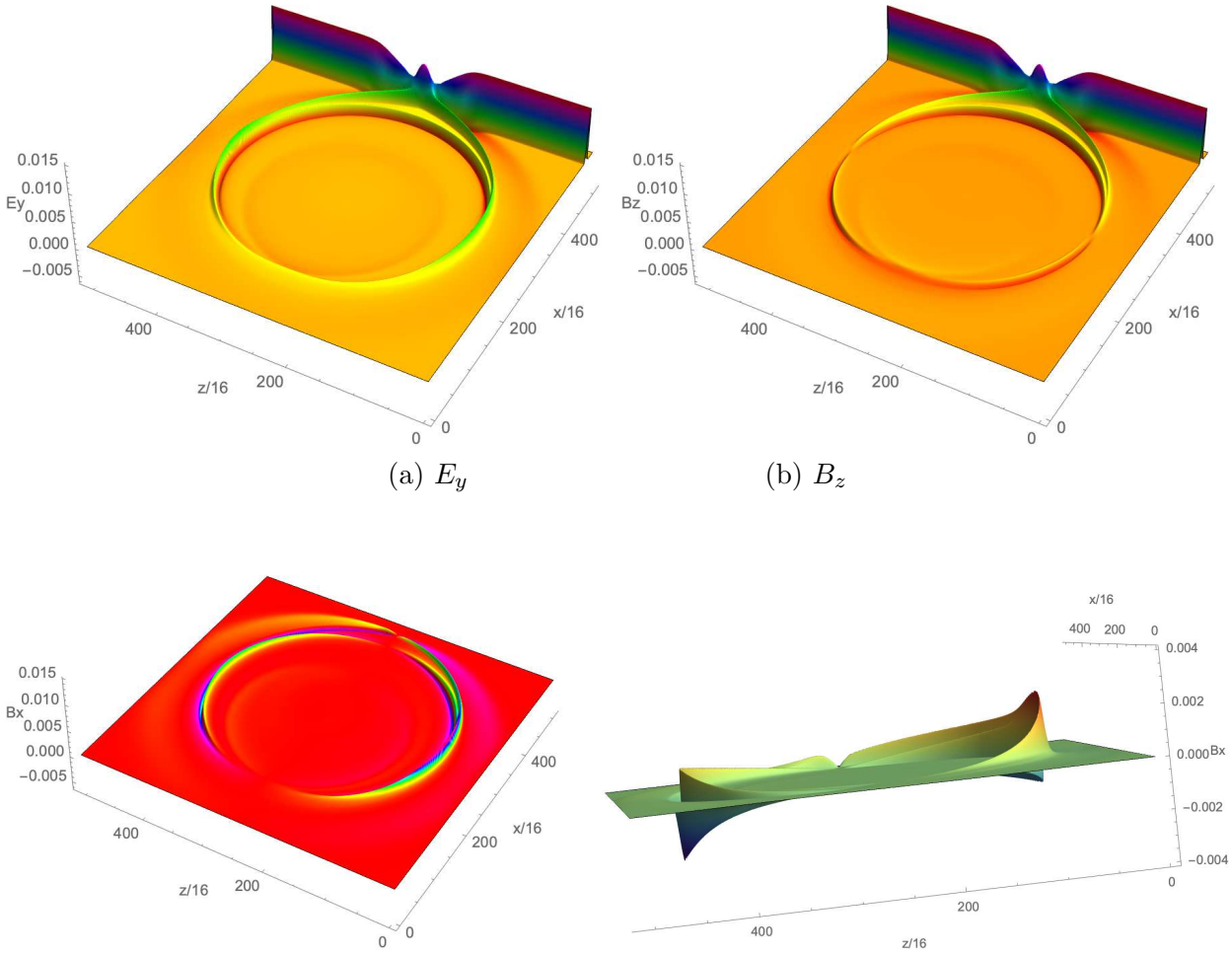

(a) E_y (b) B_z

(c) B_x (d) B_x , showing its dipole structure

Figure 8: *Snapshot of the three non-zero asymptotic components of the electromagnetic field (at* $t = 16000$*) (a)* E_y*, (b)* B_z *and the secondary field (c)* B_x *generated from the interaction of the electromagnetic pulse with the conical dielectric obstacle.*

6 References

[1] VAHALA, G, VAHALA, L., SOE, M., and RAM, A. K. 2020 One and Two Dimensional Quantum Lattice Algorithms for Maxwell Equations in Inhoogeneous Scalar Dielectric Media I: Theory, Rad Eff. Def. Solids (submitted)

[2] VAHALA, G, VAHALA, L, SOE, M & RAM, A, K. 2020. Unitary Quantum Lattice Simulations for Maxwell Equations in Vacuum and in Dielectric Media, arXiv: 2002.08450

[3] VAHALA, G, VAHALA, L, SOE, M & RAM, A, K. 2020. Unitary Quantum Lattice Simulations for Maxwell Equations in Vacuum and in Dielectric Media, J. Plasma Physics 86, 905860518

[4] JACKSON, J, D. 1998. "Classical Electrodynamics", 3rd Ed., (Wiley, New York)